Study of the beam-beam limit in e^+e^- circular colliders

K. Ohmi, M. Tawada, Y. Cai[1], S. Kamada, K. Oide, and J. Qiang[2]
KEK, 1-1 Oho, Tsukuba, 305-0801, Japan
[1]*SLAC, Menlo Park, CA 94025, USA and*
[2]*LBNL, Berkeley, CA 94720, USA*
(Dated: April 2, 2004)

Beam-beam effects limit the luminosity of circular colliders. Once the bunch population exceeds a threshold, the luminosity increases at a slower rate. This phenomenon is called the beam-beam limit. Onset of the beam-beam limit has been analyzed with various simulation methods based on the weak-strong and strong-strong models. We have observed that an incoherent phenomenon is mainly concerned in the beam-beam limit. The simulation have shown that equilibrium distributions of the two colliding beams are distorted from Gaussians when the luminosity is limited. The beam-beam limit is estimated to be $\xi \sim 0.1$ for a B factory with damping time of several thousand turns.

PACS numbers:

High luminosity B factories, PEP-II and KEKB, have been operated successfully at SLAC and KEK, respectively. There are plans to reach a higher luminosity of 10^{35} to 10^{36} $\mathrm{cm}^{-2}\mathrm{s}^{-1}$ for these B factories. We have studied how the high luminosity can be achieved. The work is directly related to understanding the beam-beam limit. The beam-beam limit is characterized by the beam-beam parameter (ξ)

$$\xi_{\pm,x(y)} = \frac{N_{\mp} r_e}{2\pi\gamma_{\pm}} \frac{\beta_{x(y),\pm}}{\sigma_{x(y),\mp}(\sigma_{x,\mp} + \sigma_{y,\mp})}, \qquad (1)$$

where $\gamma_{\pm}$, $N_{\pm}$, $\sigma_{x(y),\pm}$ and $\beta_{x(y),\pm}$ are the relativistic factor, bunch populations, the horizontal (vertical) size and beta function of positron/electron beam, respectively. The beam-beam parameter is regarded as the incoherent tune shift of the beam, which interacts with the other beam. The beam-beam parameters, which consist of four values: i.e., vertical/horizontal and positron/electron beams, correspond to the shift of betatron tune (the phase advance in a revolution) in each direction and in each beam. In the formulae, particles in the beam are assumed to have a Gaussian distribution.

The beam-beam limit is understood empirically to occur when the beam-beam parameter or tune shift is saturated at a certain value as the bunch population increases[1]. It is explained physically with the enlargement of beam due to increasing the beam-beam parameter.

The beam-beam limit can be caused by various factors. The lattice map affects the beam-beam performance. Its linear part consists of Twiss parameters and dispersion functions at the interaction point (IP). If the dispersion and/or $x - y$ coupling at the IP are nonzero, the normal coordinate of the lattice map does not match that of the beam-beam force, with the result that the luminosity is degraded. The crossing angle is equivalent to a kind of dispersion function at the IP. A nonlinear map, chromaticity, amplitude dependent tune shift and resonance structure of the lattice also affect the beam-beam limit [2–4]. In this paper we focus on the essentials of the beam-beam interaction itself, neglecting the lattice effects. The physics system of the two colliding beams is described by a smaller number of parameters: tune, damping and diffusion rate due to the synchrotron radiation, the nominal beam-beam parameters, and additionally σ_z/β_y, if we consider the bunch length.

The radiation damping time is about several thousand turns in B factories, while it is several ten or hundred thousand turns in τ-charm and ϕ factories, and is even longer in proton machines. In higher energy ($E \gg 10$ GeV) colliders such as LEP, it is several hundred turns or less. Colliders with faster damping time tend to achieve higher beam-beam parameters. In this paper, we focus on the beam-beam limit for B factories with damping time of several thousand turns.

The beam-beam limit has been studied with a two-dimensional strong-strong simulation in Ref. [5]. The beam-beam interaction of two bunches without considering their length was treated in the simulation. A coherent π mode instability was induced for $\xi > 0.05$, with the result that beam size enlargement and a luminosity limit were seen.

We studied the beam-beam limit with three-dimensional strong-strong simulations using a code named BBSS. The behavior of the beam-beam limit is somewhat different from that in the two dimensional simulation. The coherent π mode disappears and an incoherent effect dominates for the beam-beam limit: i.e., the beam-beam limit is determined by the equilibrium distribution of the two beams. The incoherent beam-beam limit is examined with parameters of super KEKB as is shown in Table 1.

The algorithm for the simulation is presented in Ref. [5, 6]. The solver is based on the particle-in-cell (PIC) method in two-dimensional grid space as is adopted in some beam-beam simulation codes [7–9]. This simulation code can also evaluate the beam-beam interaction with an analytical formula assuming a Gaussian beam distribution. The extension to three-dimensional space is basically done by slicing a bunch along the z direction. Interactions between pairs of slices are done in two-dimensional space. Particles in a bunch move across

TABLE I: The design parameters of super KEKB (tentative)

		HER	LER
Circumference	C	3,016 m	
Energy	E	8.0 GeV	3.5 GeV
Bunch population	N_e	5.5×10^{10}	1.26×10^{11}
Beta function at IP	β_x^*/β_y^*	0.30/0.003 m	
Emittance	$\varepsilon_x/\varepsilon_y$	24/0.18 nm	
Bunch length	σ_z	3 mm	
Synchrotron tune	ν_s	0.02	
Betatron tune	ν_x/ν_y	0.508/0.55	
Radiation damping time	τ_{xy}/T_0	4,000	6,000

the longitudinal slices due to the synchrotron oscillation. When the vertical beta function is comparable with the bunch length, the transverse kick of particles experiences a discontinuity at the crossing between two slices, with the result that strong numerical noise occurs. To reduce the longitudinal discontinuity, an interpolation of the potential [6, 10] was done.

In the simulation, particles were initialized as a Gaussian distribution derived from the design emittance and beta functions. The radiation damping and excitation are applied along the normal mode. A bunch is represented by 100,000 macro-particles per bunch and is divided into 5 longitudinal slices. The transverse plane is divided into 128 × 256 grids with unit size of 20μm × 0.2μm. The simulation gives an equilibrium distribution of the two beams, $\rho_+(x,y,z;s)$ and $\rho_-(x,y,z';s)$, at the interaction point $s=0$ after tracking the macro-particles during several damping times. The luminosity is estimated by the equilibrium beam distribution as follows,

$$L = f_{rep}\int \rho_+(x,y,z;s)\rho_-(x,y,z';-s)dxdydzdz' \quad (2)$$

where f_{rep} is the repetition frequency and the integration is performed keeping $s=(z-z')/2$.

Figure 1 shows evolutions of the luminosity, vertical rms beam sizes and kurtosis ($\langle y^4\rangle/3\langle y^2\rangle$). The luminosity decreases to about a half of the geometrical value 1×10^{32} cm^{-2}s^{-1} at the design parameter. Simultaneously, the vertical rms beam sizes are enlarged three to four times. The size enlargement does not reflect the luminosity drop, because the tail part of the distribution grows. The vertical kurtosis in picture (c), which characterizes the shape of the distribution, is obtained to be $3\sim5$. The horizontal beam size is shrunk by the dynamical beta and emittance effects as expected. The horizontal kurtosis had a similar value, $3\sim5$. Luminosity evolutions for various bunch populations (100%, 80%, 60%, 40% and 20% of the design) are also shown in Picture (a). Sudden dips were seen in high bunch populations (80% and 60%). Such dips are sometimes seen for different numerical conditions: i.e., grid size, initial particle distribution, the slice number and macro-particle number. The dips occurred irregularly but the luminosity and beam size finally settled on unique values. They were not seen in the Gaussian approximation.

Figure 2 shows the beam-beam parameter and the beam sizes for various currents (nominal beam-beam parameter). The luminosities were obtained by integrating the beam distributions up to 30,000 revolutions ($\approx 5\times\tau/T_0$). Since the particle distribution is distorted from a Gaussian, the calculated r.m.s size is not reflected in the luminosity; therefore the beam-beam parameter is estimated from the luminosity as follows,

$$\xi_y = \frac{2r_e\beta_{y,\pm}}{N_\pm\gamma_\pm f_{rep}}L. \quad (3)$$

where the horizontal size is kept constant, and $\sigma_x \gg \sigma_y$ is assumed. ξ calculated by Eq.(3) and ξ calculated by Eq.(1) using the design beam sizes are called the beam-beam parameter and the nominal beam-beam parameter, respectively in this paper. (The nominal parameters are calculated for $\varepsilon_x = 18$ nm here, because the horizontal size is shrunk about 80%. The design parameter corresponds to the nominal value of 0.2.)

The results given by the Gaussian approximation and by the PIC method are very different. Remarkable enlargement was not seen in the horizontal beam size, but was seen in the vertical beam size. The enlargement given by the PIC method was stronger than that by the Gaussian approximation. The Gaussian approximation gave a high beam-beam parameter of more than 0.2, while the PIC method gave saturation of the beam-beam parameter around 0.1. No significant coherent motions were seen in the first and second moments: $\langle x_i\rangle$ and $\langle x_ix_j\rangle$ in both methods. The weak-strong simulation with a Gaussian fixed beam [11] gave similar results as the Gaussian strong-strong simulation.

These different features between the PIC simulation and the Gaussian approximation, where the sudden dips are seen, give us a hint of what might be the origin of the beam-beam limit. Figure 3 shows the variation of the particle distribution during the sudden change of the luminosity. Both electron and positron distributions are depicted in the figure. Both distributions are enlarged and distorted from a Gaussian simultaneously while overlapping with each other. The final distributions after 35,000 turns are seen in Figure 3(b). The distribution of positrons is slightly broader than that of electrons, due to the difference in the radiation damping times. Both distributions, which are distorted from a Gaussian mainly in the tail part, are considered as an equilibrium distribution of the two colliding beams.

We now think that the beam-beam limit is determined by the equilibrium distribution of the two beams, but is not caused by coherent motion. To confirm this idea, we carried out a weak-strong simulation using the particle distribution obtained by the strong-strong simulation. If the beam size enlargement is due to an incoherent phenomenon, the same results of luminosity and size should be obtained in the final stage. The strong beam, which is the electron beam in the figure, is given by the final distribution of the strong-strong simulation using the

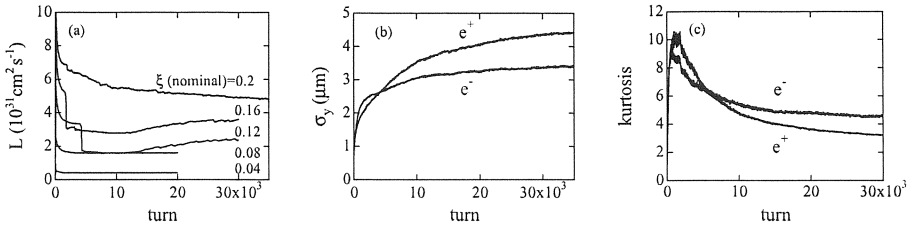

FIG. 1: Evolution of luminosity, vertical rms beam size and kurtosis ($\langle y^4\rangle/3\langle y^2\rangle$) obtained by the strong-strong simulation.

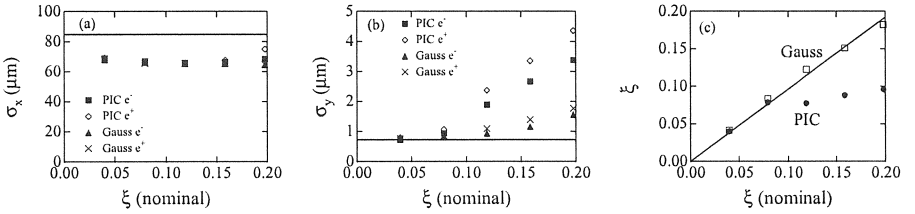

FIG. 2: Beam sizes and the beam-beam parameter function of the nominal beam-beam parameter obtained by the strong-strong simulations with the particle-in-cell method and Gaussian approximation. Horizontal and vertical beam sizes are depicted in (a) and (b). Effective beam-beam parameters are depicted in (c).

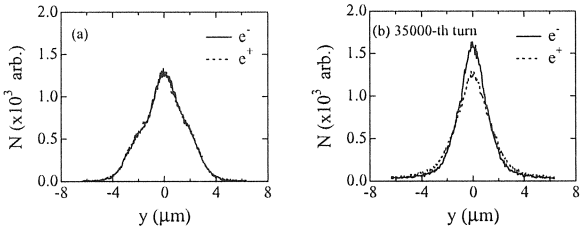

FIG. 3: Evolution of the vertical distribution of electron and positron beams. The distributions during the sudden change and after 35,000 turns are depicted in picture (a) and (b), respectively.

PIC code, while the weak positron beam is initialized with the designed Gaussian distribution. Figure 4 shows the evolution of luminosity and beam size given by the weak-strong simulation. The luminosity is at a similar level after 40,000 turns as that of the strong-strong simulation as is shown in Figure 4(a). The evolution of the beam sizes for this weak-strong simulation in Figure 4(b) is compared with Figure 1 (b). The size of the positron beam in the two simulations grows to the closed value. The two luminosities do not coincide perfectly, but have a difference of 15%. Figure 4 (c) shows the evolution of the size of the positron beam that interacts with a fixed Gaussian electron beam. The beam size is much less than that for the distorted beam. This means that the distortions are cooperative and/or destructive to each other: if one beam is distorted from a Gaussian, the other beam is forcefully distorted as well.

The beam-beam limit due to coherent motion was seen in the two-dimensional simulation [5]. In the three dimensional simulation, the coherent motion was not seen for our parameters, but was seen in the case of short bunch length, $\sigma_z < \beta_y/2$. The coherent motion disappeared at $\sigma_z = 1.5$ mm, where the results were verified for the number of slices 5 and 10 [12]. Perhaps the coherent motion is smeared due to tune spread along z in a bunch; therefore the incoherent beam-beam limit dominates.

We consider how the equilibrium distribution is formed. The beam-beam interaction is a multi-dimensional and a nonlinear dynamical system, which has the characteristic of diffusion [13]. These characteristics are different from that of a potential well distortion, which is determined by Haissinski [14, 15] or Vlasov equations. In a solvable model, the equilibrium distribution is determined by the ratio of the damping and diffusion rate due to the synchrotron radiation, namely emittance. In the beam-beam system that may be an unsolvable system. The diffusion due to nonlinearity plays an important role in determining the beam distribution. This discussion has been applied to a halo formation due to the beam-beam interaction with a weak-strong model [16]. Here we emphasize the diffusion for the two interacting beams to explain the beam-beam limit.

We emphasized an incoherent beam-beam limit in this paper. The behavior may depend on tune. In our experience, this tune operating area is the best in the tune space. Therefore it is important to understand the origin of the beam-beam limit at this tune operating point.

Horizontal and vertical tunes were surveyed in the area of $0.5 < \nu_{x,y} < 0.7$. A horizontal coherent instability dominated at the region $\nu_x > 0.55$, with the result that the beam-beam parameter went down to ~ 0.01 at the

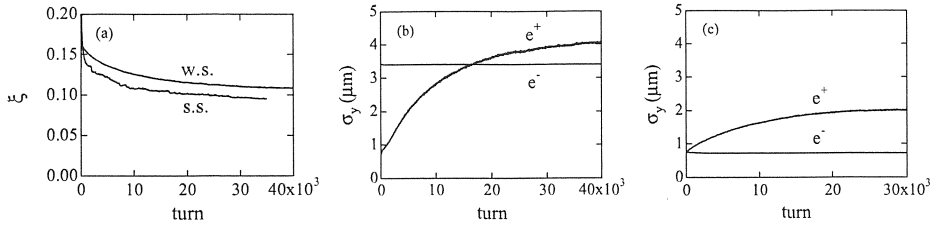

FIG. 4: Evolution of the beam-beam parameter and vertical size of electron and positron beams. Evolutions of ξ for the weak-strong and strong-strong simulation is depicted in (a), where the final distribution of the strong-strong simulation is used as a fixed distribution in the weak-strong simulation. Evolution of the beam size for the weak-strong simulation is depicted in (b). Evolution of the size of positron beam that interacts with fixed Gaussian electron beam is depicted in (c).

beam current. Vertical coherent instability was not seen in this area. The horizontal kurtosis increased > 6 when leaving the half integer line ($\nu_x \sim 0.52$-0.53), while the vertical kurtosis decreased to be < 2. Higher vertical tune ($\nu_y \sim 0.58$) showed a better beam-beam parameter $\xi_y > 0.12$. It was sensitive to the damping time of the two rings. Fourier analysis showed horizontal π mode spectra when leaving the half integer line, and broad spectra at the bare tunes in vertical.

We studied the beam-beam limit with various simulation methods: weak-strong and strong-strong models with the Gaussian approximation and the particle-in-cell method. The beam-beam limit, $\xi \sim 0.1$, was obtained by the particle-in-cell method for B factories. The beam-beam limit is determined by an equilibrium distribution of the two colliding beams, which is distorted from a Gaussian distribution. The weak-strong simulation with the distorted distribution also gave a similar beam-beam limit.

The weak-strong and strong-strong simulations with Gaussian approximation gave a higher beam-beam limit > 0.2. The Gaussian approximation is not appropriate, if we consider the mechanism of the beam-beam limit discussed above. It should be emphasized that the result of weak-strong simulation with the Gaussian approximation is quite correct: that is, if one beam is kept Gaussian with a technique, for example using beam-beam compensation, the beam-beam limit may be boosted up to $\xi > 0.2$.

We had a 15% discrepancy in the strong-strong and weak-strong simulations with the distorted distribution. The discrepancy may be due to correlations of motions of the two beams, namely, coherent motion like small breathing or others. This remains as an open question.

We only need the equilibrium distribution of the two colliding beams to understand this type of beam-beam limit. A more concise method can be applied for this purpose; for example a quasi-strong-strong simulation with the PIC method may make it easier to obtain a solution with a longer damping time[17].

The beam-beam halo, which affects the beam life time, has been estimated by weak-strong simulations with a Gaussian strong beam. We discussed the fact that the beam-beam limit of luminosity was caused by distortions of the beam distributions. The halo should also be estimated with the distorted distribution.

The authors thank members of the super KEKB design group for fruitful discussions. This work is supported by the Japan-US collaboration plan. The authors (K.O. and M.T.) thank the staffs of SLAC and LBNL for their hospitality during their stay. They are grateful to the KEK computing center for supercomputer support. This work was partially supported by the Department of Energy under Contract No. DE-AC03-76SF00515.

[1] J. T. Seeman et al., IEEE Trans. Nucl. Sci. **30**, 2033 (1983).
[2] K. Ohmi, in *Proceedings of the 2000 Euro. Part. Accel. Conf.* (2000), pp. 433–435.
[3] M. Tawada, K. Ohmi, and Y. Funakoshi (to be published).
[4] Y. K. Ohmi, M. Tawada, Proceeding of Beam-beam 2003 (2003).
[5] K. Ohmi, Phys. Rev. E **62**, 7287 (2000).
[6] K. Ohmi, M. Tawada, and K. Oide, in *Proceedings of PAC03* (2003).
[7] Y. Cai, A. W. Chao, S. I. Tzenov, and T. Tajima, Phys. Rev. ST Accel. Beams. **4**, 011001 (2001).
[8] E. B. Anderson and J. T. Rogers, in *Proceedings of a Workshop on beam-beam effects in circular colliders*, edited by T. Sen and M. Xiao (2001), vol. FERMILAB-Conf-01/390-T, p. 136.
[9] J. Qiang, M. Furman, and R. Ryne, Phys. Rev. ST Accel. Beams **5**, 104402 (2002).
[10] K. Hirata, H. Moshammer, and F. Ruggiero, Particle Accelerators **40**, 205 (1993).
[11] K. Ohmi, in *Proceedings of PAC03* (2003).
[12] K. Ohmi, M. Tawada, and K. Oide, KEK Preprint 2003-111 (2004).
[13] J. K. Koga and T. Tajima, Phys. Rev. Lett. **72**, 2025 (1994).
[14] J. Haissinski, Nuovo Cimento **18B**, 72 (1973).
[15] K. Hirata, Phys. Rev. D **37**, 1307 (1988).

[16] J. L. Tennyson, in *Proceedings of Physics of High Energy Particle Accelerators* (Batavia, 1981), pp. 345–394.
[17] K. Ohmi, K. Hirata, and N. Toge, in *Proceedings of EPAC96* (1996), pp. 1164–1166.